

PAPER • OPEN ACCESS

Developing Highly Porous Glass Microspheres via a Single-Stage Flame Spheroidisation Process

To cite this article: N A Nuzulia *et al* 2022 *J. Phys.: Conf. Ser.* **2243** 012005

View the [article online](#) for updates and enhancements.

You may also like

- [A Comparative Study of Production of Glass Microspheres by using Thermal Process](#)
May Yan Lee, Jully Tan, Jerry YY Heng *et al.*
- [Polymer-coated microparticle scaffolds engineered for potential use in musculoskeletal tissue regeneration](#)
Gelareh Samandi, Vineet Gupta, Neethu Mohan *et al.*
- [Composite design bioinspired by the mesocarp of Brazil nut \(*Bertholletia excelsa*\)](#)
M Sonogo, V F Sciuti, R Vargas *et al.*



ECS Membership = Connection

ECS membership connects you to the electrochemical community:

- Facilitate your research and discovery through ECS meetings which convene scientists from around the world;
- Access professional support through your lifetime career;
- Open up mentorship opportunities across the stages of your career;
- Build relationships that nurture partnership, teamwork—and success!

Join ECS!

Visit electrochem.org/join



Developing Highly Porous Glass Microspheres via a Single-Stage Flame Spheroidisation Process

N A Nuzulia^{1,2}, Md T Islam^{3,4}, A Saputra², T Sudiro⁵, G E Timuda⁵, T Mart^{1*}, Y W Sari², and I Ahmed³

¹ Department of Physics, Faculty of Mathematics and Natural Sciences, Universitas Indonesia

² Department of Physics, Faculty of Mathematics and Natural Sciences, IPB University

³ Advanced Materials Research Group, Faculty of Engineering, University of Nottingham

⁴ Department of Applied Chemistry and Chemical Engineering, Faculty of Engineering, Noakhali Science and Technology University, Noakhali-3814, Bangladesh

⁵ Research Center for Physics, Indonesian Institute of Sciences, Indonesia

*Email:terry.mart@sci.ui.ac.id

Abstract. Glass microspheres are gaining attention in bone tissue engineering due to their ability to convert into hydroxyapatite-like materials, resembling the inorganic mineral of natural bone. The morphology of glass microspheres as starting material has been considered to influence the conversion rate and the resulting product where porous microspheres could promote faster conversion to hydroxyapatite than solid microspheres. This paper reports on manufacturing glass microspheres (solid and porous) using a flame spheroidisation process. The effect of various gas ratios of acetylene and oxygen on the morphological changes of glass microspheres was investigated. Irregular shaped glass particles with starting particle size ranges of 63 – 125 μm were used as feed and delivered to a hot flame to produce solid microspheres. To manufacture porous glass microspheres via a single-stage flame spheroidisation process, calcium carbonate was utilised as a porogen and mixed with the glass particles. Solid and porous glass microspheres were successfully produced, exploring various gas ratios of 3:3, 4:7, 5:7 and 6:7 with a mean particle size range between 73 – 105 μm . Moreover, the average pore size of 6 μm and 9 μm was obtained using 5:7 and 6:7 gas ratios, respectively. This single-stage flame spheroidisation process is a promising method for producing both solid and porous bioactive glass microspheres.

1. Introduction

In biomedical engineering, the success of biomaterials is related to the material's ability to interact with living cells or to bond actively with surrounding tissue [1]. Glasses such as silicate-based and borate-based glasses are among the most studied biomaterials due to their ability to convert partially or entirely into hydroxyapatite-like materials [2]. Later, hydroxyapatite-like materials converted from glasses could bond actively to the surrounding hard tissue and soft tissues [3]. Pre-clinical study in a rat calvarial defect [4, 5] and rabbit femoral condyle model [6] showed that glass scaffold or injectable glass particles converted to hydroxyapatite (HA) could enhance new bone formation and regeneration. In addition, another in vitro and in vivo study trialled the use of glass microfibers doped with copper (Cu) as a wound dressing. The results revealed that Cu-doped glass microfibers converted to HA had a better capacity to stimulate angiogenesis and accelerate the healing of the full-thickness skin wounds in rodents [7].



In bone tissue regeneration, bioactivity and surface reactivity of hydroxyapatite materials could be increased by modifying their morphology and geometry. One of the most widely studied is the development of microspheres, the 3D spherical particles ranging from 1 μm to 1000 μm [8]. Microspheres exhibit greater advantages over irregular shaped particles such as larger surface area, which are beneficial to increase surface reactivity with surrounding tissue and cellular responses resulting in better-facilitating bone tissue engineering [9, 10]. Moreover, porous microspheres with interconnected porosity offer further advantages over solid microspheres, such as improved good flow properties facilitating minimally invasive injection procedures for ease of delivery to specific target areas [11]. In this case, hydroxyapatite microspheres converted from the glass are considered as a novel class of scaffold materials with controllable conversion rates to hydroxyapatite within phosphate-rich media [12]. The study showed that the external product dimensions of hydroxyapatite converted from glass was nearly identical to that of starting materials known as pseudomorphic reaction [13, 14].

For producing microspheres, several methods have been applied for such as acid-catalyzed sol-gel method [9], template-assisted hydrothermal [15], spray pyrolysis [16], solvent evaporation [10] and flame spray spheroidisation [12, 17–20]. The flame spheroidisation method has been developed as an effective method to produce solid microspheres [21]. In addition, this method has been developed further as a single-stage manufacturing process for producing porous glass microspheres [12, 18–20, 22]. Some important parameters influence the production of microspheres comprising of physical properties such as the glass material and particle size, properties of the flame (temperature of flame and pressure of gas) and process parameters (particle feed rate into the flame) [19, 23]. A modelling study of microspheres production showed that the glass particles with a size greater than 200 μm were not spheroidised due to the greater density resulting in incomplete spherical shape particles. Unspheroidised particles may have been caused by insufficient heat exchange kinetics for the particle to reach the required temperature to melt the glass particles [23]. In the flame spheroidisation method various gas carriers have been used such as pure oxygen [21], propane [17], argon [24] and oxygen/acetylene [12, 17–19, 25, 26]. Among those gases, oxygen/acetylene has been widely used as it produces higher flame temperature [27] and has been shown to produce smooth spherical particles successfully. This paper reports on the effect of oxygen/acetylene gas ratio on the flame quality and how it influences the morphology of solid and porous glass microspheres fabricated using flame spheroidisation method.

2. Materials and Method

2.1 Preparation of glass particles

Glass particles were prepared following the method in the previous study [12] by using boron oxide (B_2O_3), phosphorus pentoxide (P_2O_5), sodium carbonate (Na_2CO_3), and calcium carbonate (CaCO_3) as starting materials (Sigma Aldrich, U.K). The precursors were placed into a platinum-rhodium alloy crucible (Birmingham Metal Company, U.K.) and dried in the furnace with $10^\circ\text{C min}^{-1}$ ramp to 350°C for 0.5 hours to remove any residual moisture then raised to 800°C for 0.5 hours to remove CO_2 . The sample was then melted at 1150°C for 1.5 hours. The resulting molten glass was quenched between two steel plates and allowed to cool to room temperature. The glass particles were then ground using a ball mill (Retsch PM 100) and sieved into the particle size range of 63 – 125 μm .

2.2 Fabrication of glass microspheres

Fabrication of glass microspheres was performed using glass particles with a size range of 63 – 125 μm . Solid microspheres (SGMs) were produced by delivering the glass particles as a feed into the hot flame via flame spheroidisation method utilising oxy/acetylene flame spray gun (MK 74, Metallisation Ltd, UK). Various gas ratios of acetylene: oxygen was trialled at 3:3, 4:7, 5:7 and 6:7.

For porous microspheres (PGMs), calcium carbonate porogen was added to the glass particle at a ratio of 3:1 as described elsewhere and processed via a single-stage process through flame spheroidisation similar to SGMs [12]. After manufacturing, the porous microspheres were collected

from the cooling tray, washed gently in deionized water for 1 minute to remove residual calcium carbonate porogen and dried at 50°C for 24 hours in a drying oven.

2.3 Surface morphology characterization

The surface morphology of microspheres (solid and porous) was examined using a scanning electron microscopy (SEM JEOL JSM-IT200) operated at 15kV. The particle size of the microspheres as determined from SEM micrograph was measured using Fiji ImageJ. In addition, energy dispersive x-ray analysis (EDX) was carried out to confirm the elemental composition.

3. Results

3.1 Surface morphology and chemical composition of bulk glass particles

The morphology of the bulk glass particles prepared using the melt-quench method is shown in Figure 1, revealing their irregular-shaped nature. The particles size is less than 125 μm . Selection on the particle size range of 63 – 125 μm was referred to in the previous study that was reported to be the optimum size of starting glass for manufacturing spheroidized particles. The EDX analysis presents the actual composition of glass compared with the expected composition that is shown in Table 1.

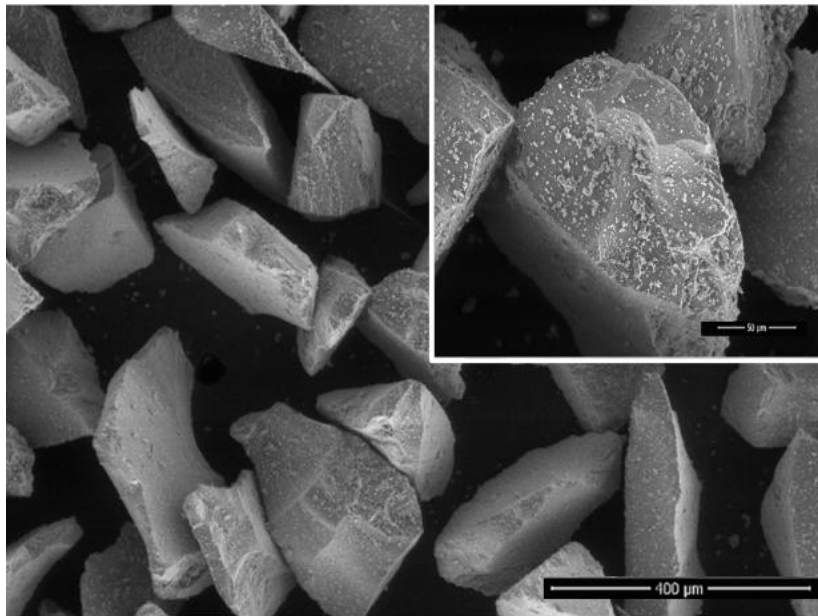


Figure 1. Morphology of bulk glass particles.

Table 1. Composition of bulk glass particles

Glass Code	Composition (mol%)			
	P ₂ O ₅	Na ₂ O	CaO	B ₂ O ₃
BG particles (expected)	1.7	22.7	21.8	53.8
BG particles (actual)	3.6	36.5	48.6	

3.2 Flame spheroidisation

The flame properties consisting of flame colour and length were observed alongside varying the acetylene and oxygen gas ratio, as highlighted in Table 2. The flame colour changed from red to blue when the gas ratio was increased from 3:3 to 6:7. Meanwhile, the flame length was observed at approximately 190 mm length for the gas ratio 3:3 with red colour flame. The flame length was seen to decrease (from 190 mm to 115 mm) with the increase in gas ratio from 3:3 to 5:7. On the other hand, the gas ratio of 6:7 resulted in a similar flame length to that of 3:3 gas ratio.

Table 2. Flame colour and length of various acetylene and oxygen gas ratio

Acetylene : Oxygen Gas Ratio	Flame Colour	Flame Length (mm)
3 : 3	Red	190
4 : 7	Blue	125
5 : 7	Blue	115
6 : 7	Blue Bright	182

3.3 Surface morphology and chemical composition of glass microspheres

The morphology of the glass microspheres after flame spheroidisation are shown in Figure 2. Solid glass microspheres (SGMS) and porous glass microspheres (PGMS) were successfully produced via the flame spheroidisation in all acetylene and oxygen gas ratios except for PGMS with a 3:3 gas ratio. Figure 2 shows smooth and spherical glass microspheres, especially for SGMS with a 3:3 and 6:7 gas ratio. Moreover, the SEM results represent the formation of pore morphologies utilising a single-stage process, and the yield of pore achieved increased with the increase of gas ratio from 4:7 to 6:7.

The particle size distribution was measured using Fiji ImageJ and presented in Table 3. As can be seen from Table 3, the mean particle size ranges were 83 – 105 μm for SGMS and 73 – 101 μm for PGMS. Moreover, mean pore sizes for PGMS were found to be $6 \pm 3 \mu\text{m}$ and $9 \pm 5 \mu\text{m}$ for 5:7 and 6:7 gas ratio, respectively.

The EDX analysis shows changes in glass composition before and after spheroidisation (Table 4). The results identify the composition of P_2O_5 , Na_2O and CaO both in SGMS and PGMS. Nevertheless, the composition of B_2O_3 is only identified in SGMS because boron is the light element that could not be easily detected using EDX.

Table 3. Mean particle size of solid and porous glass microspheres with various acetylene/oxygen gas ratio

Acetylene : Oxygen Gas Ratio	SGMS (μm)	PGMS (μm)
3 : 3	105 ± 18	83 ± 23
4 : 7	86 ± 8	73 ± 15
5 : 7	91 ± 14	94 ± 13
6 : 7	83 ± 12	101 ± 13

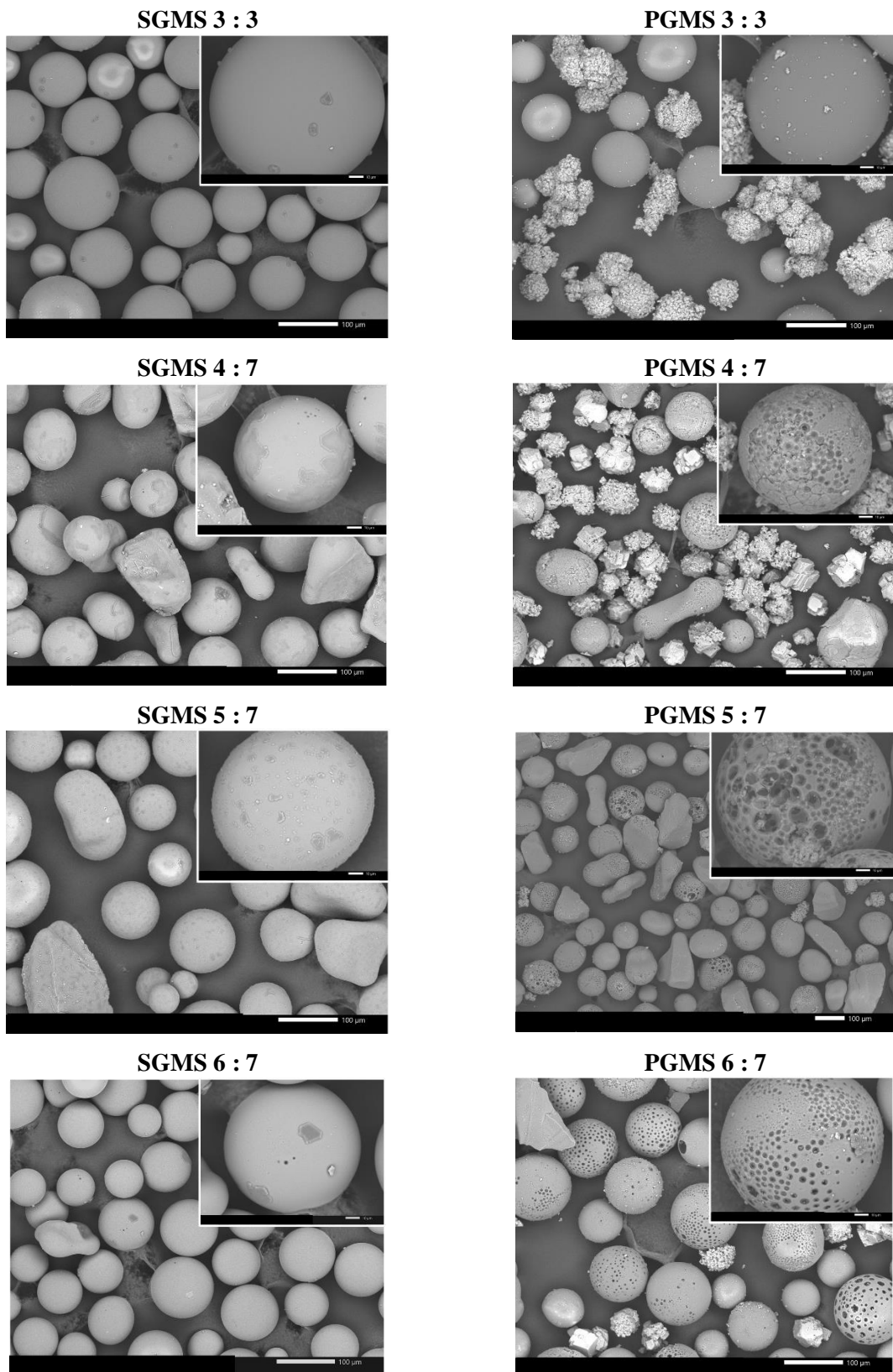


Figure 2. SEM images of solid and porous glass microspheres with various acetylene and oxygen gas ratio (3:3, 4:7, 5:7 and 6:7)

Table 4. Composition of solid and porous glass microspheres

Acetylene : Oxygen ratio	Glass form	Composition (mol%)			
		P ₂ O ₅	Na ₂ O	CaO	B ₂ O ₃
Expected		1.7	22.7	21.8	53.8
3 : 3	SGMS	2.1	25.9	22.6	60.5
	PGMS	1.0	21.6	16.4	72.4
4 : 7	SGMS	1.7	20.5	25.2	51.4
	PGMS	6.3	29.7	43.0	
5 : 7	SGMS	1.1	23.2	12.1	61.0
	PGMS	3.4	34.8	54.5	
6 : 7	SGMS	1.6	22.2	18.0	61.6
	PGMS	3.8	9.1	94.8	

4. Discussion

The flame spheroidisation process has recently been developed to be a single-stage process to produce porous glass microspheres by varying the gas ratio of acetylene and oxygen. The particle size of starting material plays an important role to produce spherical particles. A previous study reported that most spherical particles were obtained using the initial particle sizes of 45 – 200 μm [19]. In this study, the starting bulk glass particles were in the size range of 63 – 125 μm to prepare solid glass microspheres (SGMS) and porous glass microspheres (PGMS). Those starting glass particles sizes successfully produced highly porous glass microspheres using 3:1 porogen to glass powder ratio [12]. The previous study showed that those initial glass particle sizes successfully produced porous phosphate glass microspheres with the interconnected pores performing osteogenic potential assessed in 13 weeks implantation with ovine bone defect model [28].

In flame spheroidization, the flame's temperature is critical for producing microspheres [23] related to the energy to melt the bulk glass particles. Flame temperature can be controlled by the fuel gas used to create a flame, where oxygen/acetylene could produce a higher flame temperature to fabricate smooth spherical particles [27]. In addition, flame properties such as flame colour and length have been considered as another factor influencing the fabrication of microspheres that can be adjusted with the gas ratio variation of acetylene (combustible gas) and oxygen (combustion-supporting gas). In this study, the flame colour changed from red to blue bright when the gas ratio was increased from 3:3 to 6:7, as shown in Table 2. The higher gas ratio used to create flame tends to increase the pressure of the combustion field and could increase the turbulent intensity of the mixture of the fuel and oxidizer [21]. Critical to the property of the flame was not only the flame colour but also the flame length. The study showed that flame length could affect the production of porous microspheres and the surface pore size [22]. As seen in Table 2, the flame length decreased from 190 mm to 115 mm with the increase in gas ratio from 3:3 to 5:7. The higher the acetylene flow rate as the fuel gas resulted in the shorter flame

length. Nevertheless, the gas ratio of 6:7 resulted in a similar flame length to that of 3:3 gas ratio as 182 mm with the blue bright flame colour. In short, the gas ratio of 6:7 could be the optimum flame for manufacturing glass microspheres, among others, due to the bright blue colour with a long flame length.

As the gas ratio of acetylene and oxygen influenced the property of the flame, it also affected the manufacturing of glass microspheres. As seen in Figure 2, all gas ratios (3:3, 4:7, 5:7 and 6:7) successfully produced solid glass microspheres (SGMS) with the optimum result obtained using 6:7 gas ratio, as shown by the production of smooth and spherical particles in the majority. Nevertheless, there were a few particles that were not spherical for the 4:7 and 5:7 gas ratios. It might be caused by larger particle sizes and higher density of starting glass particles that require more energy supply of the acetylene/oxygen flame to be melted [23, 25]. Furthermore, Figure 2 revealed that porous microspheres were initially produced using the 4:7 gas ratio shown by pores on the surface. The pore yield and size increased with the increase of gas ratios (5:7 and 6:7). The highest gas ratio of 6:7 resulted in the most uniform porous microspheres with pore size increases observed. Meanwhile, calcium carbonate was present as a porogen in all PGMS samples shown by the coral-like particles surrounding microspheres. The incomplete washing process of PGMS might cause the presence of carbonate to remove the porogen completely.

In summary, as the gas ratio increases, the pressure of the flame increase. It will influence the surface tension effect of the in-flight particle to melt, and spheroidize the initial glass powders [25]. So, once glass powders were melted at high temperatures and cooled rapidly, the spherical shape was formed due to the surface tension [17]. This study showed that porous glass microspheres could be prepared via a single-stage flame spheroidisation with acetylene and oxygen gas ratio of 6:7.

5. Conclusions

An oxygen/acetylene flame spheroidisation process is an effective process to produce microspheres. Various gas ratios of acetylene and oxygen (3:3, 4:7, 5:7 and 6:7) flame successfully produced smooth and spherical particles of solid and porous from an irregular shaped bulk glass particles. The morphology change become more spherical particles in the majority as the gas ratio increased (from 4:7 to 6:7). Porous glass microspheres were also optimally formed using a 6:7 gas ratio with a mean particle size of 101 μm and mean pore size of 9 μm .

Acknowledgments

This work is supported by Newton Fund Institutional Link with project reference number 527323010 and Hibah Penelitian Terapan (PT) 2021 from the Ministry of Research, Technology and Higher Education Indonesia with the contract number 1/E1.KP.PTNBH/2021.

References

- [1] Bhat S V 2002 *Biomaterials* (India: Narosa Publishing House)
- [2] Rahaman MN, Day DE, Sonny Bal B, Fu Q, Jung SB, Bonewald LF, Tomsia AP 2011 *Acta Biomater* **7** 2355–2373
- [3] Hussain R, Ghafoor F, Khattak MA 2018 *3D scaffolds of borate glass and their drug delivery applications Biomedical, Therapeutic and Clinical Applications of Bioactive Glasses* (USA: Elsevier)
- [4] Bi L, Rahaman MN, Day DE, Brown Z, Samujh C, Liu X, Mohammadkhah A, Dusevich V, Eick JD, Bonewald LF 2013 *Acta Biomater* **9** 8015–8026
- [5] Gu Y, Huang W, Rahaman MN, Day DE 2013 *Acta Biomater* **9** 9126–9136
- [6] Cui X, Huang W, Zhou J, et al *Mater Sci Eng C* **73** 585–595
- [7] Zhao S, Li L, Wang H, Zhang Y, Cheng X, Zhou N, Rahaman MN, Liu Z, Huang W, Zhang C

- 2015 *Biomaterials* **53** 379–391
- [8] Noguez Méndez NA, Quirino Barreda CT, Vega AF, Miranda Calderon JE, Urioste CG, Palomec XC, Martínez AR, Díaz MP 2017 *Design and development of pharmaceutical microprocesses in the production of nanomedicine Nanostructures Oral Med* (US: Elsevier)
- [9] Lei B, Chen X, Han X, Li Z 2011 *J Mater Chem* **21** 12725–12734
- [10] Cai Y, Chen Y, Hong X, Liu Z, Yuan W 2013 *Int J Nanomedicine* **8** 1111–1120
- [11] Matamoros-Veloza A, Hossain KMZ, Scammell BE, Ahmed I, Hall R, Kapur N 2020 *J Mech Behav Biomed Mater* **102** 1-8
- [12] Islam MT, Macri-Pellizzeri L, Sottile V, Ahmed I 2021 *Biomater Sci* **9** 1826-1844
- [13] Marion NW, Liang W, Reilly GC, Day DE, Rahaman MN, Mao JJ 2005 *Mech Adv Mater Struct* **12** 239–246
- [14] Huang W, Day DE, Rahaman MN 2007 *J Am Ceram Soc* **90** 838–844
- [15] Qi YC, Shen J, Jiang QY, Jin B, Chen JW, Zhang X, Su JL 2016 *J Mater Sci* **51** 2598–2607
- [16] Sambudi NS, Cho S, Cho K 2016 *RSC Adv* **6** 43041-43048
- [17] Lee MY, Tan J, Heng JYY, Cheeseman C 2017 *IOP Conf Ser Mater Sci Eng* **205** 012022
- [18] Hossain KMZ, Patel U, Kennedy AR, Macri-Pellizzeri L, Sottile V, Grant DM, Scammell BE, Ahmed I 2018 *Acta Biomater* **72** 396–406
- [19] Gupta D, Hossain KMZ, Ahmed I, Sottile V, Grant DM 2018 *ACS Appl Mater Interfaces* **10** 25972–25982
- [20] Molinar Díaz J, Samad SA, Steer E, Neate N, Constantin H, Islam MT, Brown PD, Ahmed I 2020 *Mater Adv* **1** 3539–3544
- [21] Suzuki S, Sasaki K, Nakatsuka N, Hayashi J, Hagiwara Y, Iino K, Akamatsu F 2016 *AJTEC2011* **44** 1–7
- [22] Ahmed I, Ren H, Booth J 2019 *Johnson Matthey Technol Rev* **63** 34–42
- [23] Bortot MB, Prastalo S, Prado M 2012 *Procedia Mater Sci* **1** 351–358
- [24] Gu YW, Yap AUJ, Cheang P, Kumar R 2004 *Biomaterials* **25** 4029–4035
- [25] Jin H, Xu L, Hou S 2010 *J Mater Process Technol* **210** 81–84
- [26] Poirier T, Labrador N, Gamarra M, Enet N, Lira J 2005 *High Temp Mater Process* **9** 509-520
- [27] Shanmugam G 2000 *Basic Mechanical Engineering* (New Delhi - McGraw-Hill Publishing Company Limited)
- [28] McLaren JS, Macri-Pellizzeri L, Hossain KMZ, Patel U, Grant DM, Scammell BE, Ahmed I, Sottile V 2019 *ACS Appl Mater Interfaces* **11** 15436–15446